Technical Report Documentation Page

1. Report No.	2. Government Accession No.	3. Recipient's Catalog No.
FHWA/TX-02/1702-S		

4. Title and Subtitle	5. Report Date
DEVELOPMENT OF A PROTOTYPE HIGH-FREQUENCY GROUND-PENETRATING RADAR SYSTEM	January 2002
	6. Performing Organization Code
7. Author(s)	8. Performing Organization Report No.
Jeong-Soo Lee, Cam Nguyen and Tom Scullion	Report 1702-S
9. Performing Organization Name and Address	10. Work Unit No. (TRAIS)
Texas Transportation Institute The Texas A&M University System College Station, Texas 77843-3135	11. Contract or Grant No. Project No. 0-1702
12. Sponsoring Agency Name and Address	13. Type of Report and Period Covered
Texas Department of Transportation Research and Technology Implementation Office P. O. Box 5080 Austin, Texas 78763-5080	Project Summary: September 1997-August 1999
	14. Sponsoring Agency Code

15. Supplementary Notes

Research performed in cooperation with the Texas Department of Transportation and the U.S. Department of Transportation, Federal Highway Administration.
Research Project Title: Develop Improvements for Ground-Penetrating Radar

16. Abstract

This report describes the development of a prototype 3 GHz ground-penetrating radar (GPR) system for highway applications. The development of each subsystem, the pulse generator, the receiver, and the antenna is discussed. These components have been integrated to form a GPR prototype, which was tested in the laboratory. The results of this first GPR prototype test were promising.

Work is under way to produce a field unit. To this end, design improvements will be made to optimize the performance of all of the components. This final system will be realized using microwave integrated-circuit technology to ensure its miniaturization, low cost, and high efficiency.

17. Key Words	18. Distribution Statement
Ground-Penetrating Radar, GPR, Antenna Design, Receiver Design, Highways	No restrictions. This document is available to the public through NTIS: National Technical Information Service 5285 Port Royal Road Springfield, Virginia 22161

19. Security Classif.(of this report)	20. Security Classif.(of this page)	21. No. of Pages	22. Price
Unclassified	Unclassified	28	

Form DOT F 1700.7 (8-72) **Reproduction of completed page authorized**

DEVELOPMENT OF A PROTOTYPE HIGH-FREQUENCY GROUND-PENETRATING RADAR SYSTEM

by

Jeong-Soo Lee
Graduate Research Assistant
Department of Electrical Engineering

Cam Nguyen
Professor
Department of Electrical Engineering

and

Tom Scullion
Research Engineer
Texas Transportation Institute

Report 1702-S
Project Number 0-1702
Research Project Title: Develop Improvements for Ground-Penetrating Radar

Sponsored by the
Texas Department of Transportation
In Cooperation with the
U.S. Department of Transportation
Federal Highway Administration

January 2002

TEXAS TRANSPORTATION INSTITUTE
The Texas A&M University System
College Station, Texas 77843-3135

DISCLAIMER

The contents of this report reflect the views of the authors, who are responsible for the opinions, findings, and conclusions presented herein. The contents do not necessarily reflect the official view or policies of the Federal Highway Administration (FHWA) or the Texas Department of Transportation (TxDOT). This report does not constitute a standard, specification, or regulation, nor is it intended for construction, bidding, or permit purposes. The engineer in charge of the project was Tom Scullion, P.E. #62683.

There is no invention or discovery conceived or reduced to practice in the course of or under this contract, including any art, method, process, machine, manufacture, design, or composition of matter, or any new and useful improvement thereof, or any variety of plant which is or may be patentable under the patent law of the United States of America or any foreign country.

ACKNOWLEDGMENTS

The Texas Department of Transportation is acknowledged for its continuing interest in applying ground penetrating radar (GPR) technology to a range of pavement problems. This work would not be possible without the support and direction provided by Mr. Carl Bertrand of the Pavement Design Division of the Texas Department of Transportation (TxDOT). Funding was provided by both TxDOT and FHWA.

TABLE OF CONTENTS

Page

LIST OF FIGURES

IMPLEMENTATION RECOMMENDATIONS

Project 0-1702 has focused on enhancing TxDOT capabilities to collect, process and use GPR data. With its recent purchase of two additional GPR systems, TxDOT will be actively implementing the findings of this research project over the next few years. Specific recommendations are as follows:

With regard to district implementation of new systems:

- A new one-day training school should be developed for district data collectors. This will focus on both hardware and software aspects of data collections. The district operators will need to be taught how to use the data acquisition system RADAR2000, which was developed under Project 0-1702.
- The current GPR school notebooks should be upgraded to include descriptions of the new data collection and processing systems developed in Project 0-1702. Consideration should be given to providing district engineering staff with updated training in the most recent version of COLORMAP.

With regard to new system development:

- Project 0-1702 provided funding to build a prototype high-frequency GPR system developed for quality control applications on new flexible pavements. This system has been shown to be operational in a laboratory setting. The Texas Transportation Institute (TTI) is continuing to develop this system in-house to eventually build a unit capable of operating in the field. Once this development is complete TxDOT will be approached to evaluate this system for testing new pavement layers. If that is successful consideration should be given to provide funding to implement the system within TxDOT divisions and districts.

CHAPTER 1. INTRODUCTION AND BACKGROUND

Ground-penetrating radar has proven to be an excellent tool for nondestructive evaluation and inspection of highway structures. It has received increasingly significant attention and interest in the highway sectors, especially in the U.S., Europe, and Japan. Highway applications of GPR include identifying defects behind retaining walls and within pavements and bridge decks, locating moisture damage, and detecting the corrosion of reinforcing steel in concrete. GPR has recently been used by TxDOT to assess the thickness of pavement layers and to detect subsurface moisture-related problems in surfacing and base layers. The existing 1 GHz GPR systems, however, can provide only limited information regarding resolution, penetration, and discrimination. They are based on 25-year-old radar technology and do not make use of current advanced microwave developments. For instance, they have difficulty penetrating concrete pavements and thick structures due to insufficient power; in some cases this limits the systems' abilities to accurately determine thickness and detect defects. In addition, the existing GPR systems work at low frequencies, which result in low resolution. Furthermore, they are bulky and heavy (the existing TEM horn antennas alone typically measure 48 inch x 16 inch x 16 inch), making it very difficult or impossible to perform inspections of some materials, such as walls, the insides of pipes, or tunnel linings. These systems are normally mounted on a vehicle and used for pavement inspections. Despite the increased use and activities of GPR, no dramatic breakthrough in GPR technology for the highway practice has occurred since the original application.

To address the limitations of the existing systems, a research project has been undertaken to develop a compact high-frequency GPR for efficient and accurate detection of subsurface problems for highway applications. In this report we will describe the first prototype system, including its components and measured performance.

CHAPTER 2. GPR SYSTEM

Figure 1 shows the block diagram of the GPR prototype with its major components. It has a microprocessor-based electronic section and a microwave section. The electronic section controls the GPR's operation to perform data acquisition and processing, and to display the measured results. The heart of the GPR is the microwave section that dictates the system's performance as well as its size. It consists of a receiver, a transmitter, and receiving and transmitting antennas. The pulse generator of the transmitter generates a mono-cycle pulse of 0.33 non-second pulse width. The pulse is amplified by the power amplifier and is radiated by the transmitting antenna. The reflected signals from the surface and subsurface will go through the receiving antenna and sampling head to produce a low-frequency signal. This low-frequency signal, containing information of the subsurface conditions, is then amplified by the IF amplifier.

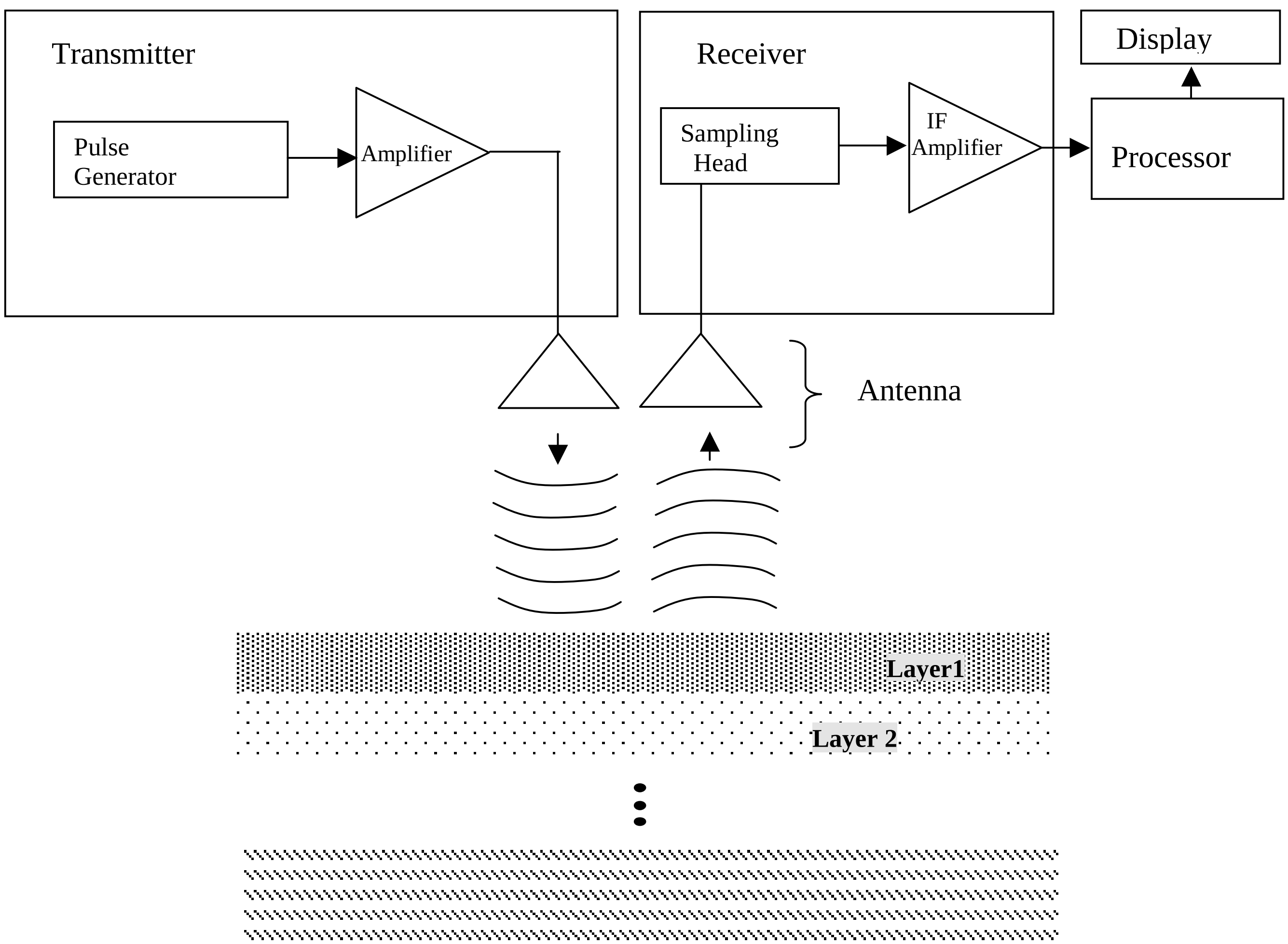

Figure 1. Block Diagram of Ground-Penetrating Radar.

CHAPTER 3. GPR COMPONENTS AND SUBSYSTEMS

3.1 Antennas

Two kinds of antenna have been developed: a small TEM horn antenna and a novel microstrip-horn antenna.

Figure 2 shows a picture of the small 3 GHz TEM horn antenna.

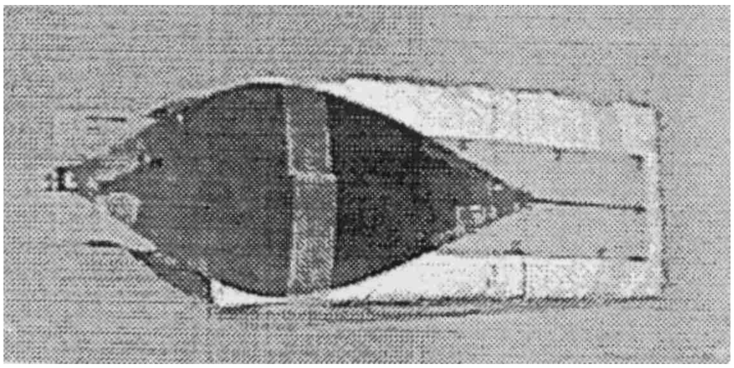

Figure 2. The Developed 3 GHz TEM Horn Antenna.

Using two identical antennas, one transmitting and one receiving, separated by a metal plate, a mono-cycle pulse of 0.33 ns width is transmitted on the transmitting antenna and the reflected pulse is captured on the receiving antenna. Figure 3 shows the reflected pulse captured using a digitizing oscilloscope. The amplitude is not the actual amplitude of the received pulse because the measurement setup used attenuators.

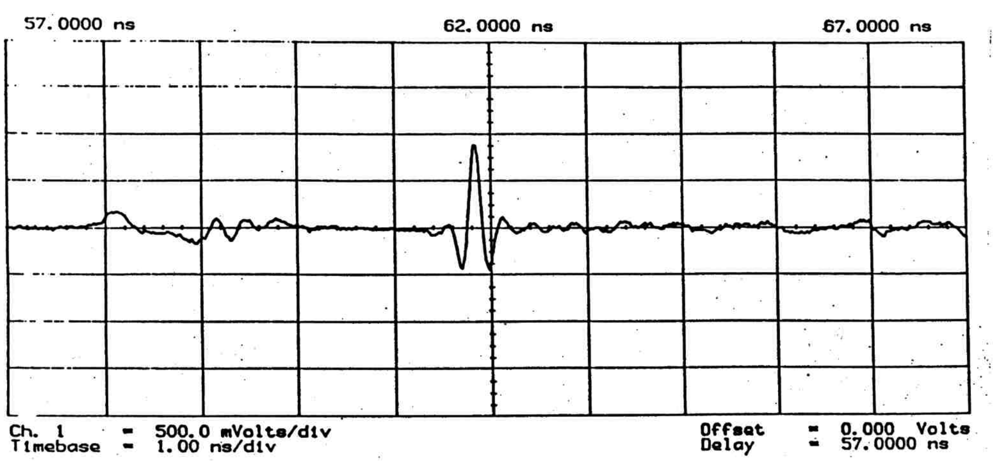

Figure 3. Received Pulse Using the 3 GHz TEM Horn Antenna.

The researchers also invented a novel ultra-wide-band antenna (*patent pending*), referred to as *microstrip-horn antenna*. As compared to existing wide-band antennas, such as the TEM horn antenna, this new antenna has many advantages:

- It possesses an extremely broad bandwidth. Our measured results indicate a bandwidth of at least 10 decades (one decade is 1:10 bandwidth). The achieved bandwidth is therefore much wider than that of the existing TEM Horn Antenna which has a typical bandwidth of about 1 decade. In fact, the new antenna's bandwidth of much wider than any wide-band antennas currently used in practice, such as the bow-tie, spiral, and log-periodic antennas. The extremely wide bandwidth capability of the new antenna allows wide-band signals, e.g., narrow pulses covering decades of bandwidth, to be transmitted and received more completely than known antennas. More power of the signal can therefore be transmitted and received. Moreover, more information reflected from the radar targets can be captured.
- No '*balun*' (balanced and unbalanced) is required. This eliminates all the disadvantages of the known TEM horn antenna in connection with its balun such as limited operating bandwidth, and increased loss. All of the current wide-band antennas, including the bow-tie, spiral and log-periodic antennas, require a balun, at the antenna input.
- There is a small coupling between the two antennas when used in a transmitting and receiving antenna system, even when they are next to each other and no absorbing material is used. This unique feature is extremely attractive for radar and sensor applications where the antennas need a certain degree of isolation between them.

The researchers designed the new antenna and obtained good results even with this first-iteration design. Figure 4 shows measured return loss of the first prototype antenna, better than 10 dB from 200 MHz to more than 20 GHz. Note that we did not measure beyond 20 GHz, but the performance trend indicates a much higher frequency than 20 GHz, which is also expected theoretically. Figures 5 and 6 show radiation patterns at 2.6 and 15 GHz, respectively. Figure 7 shows the pulse received by the new microstrip-horn antenna.

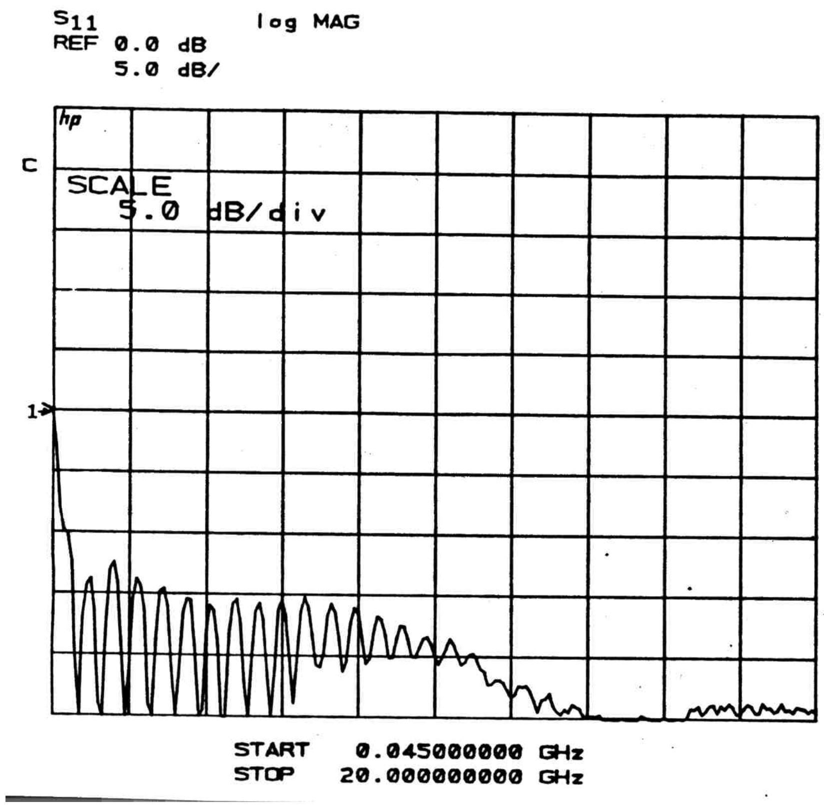

Figure 4. Measured Return Loss of the New Microstrip-Horn Antenna (First Design).

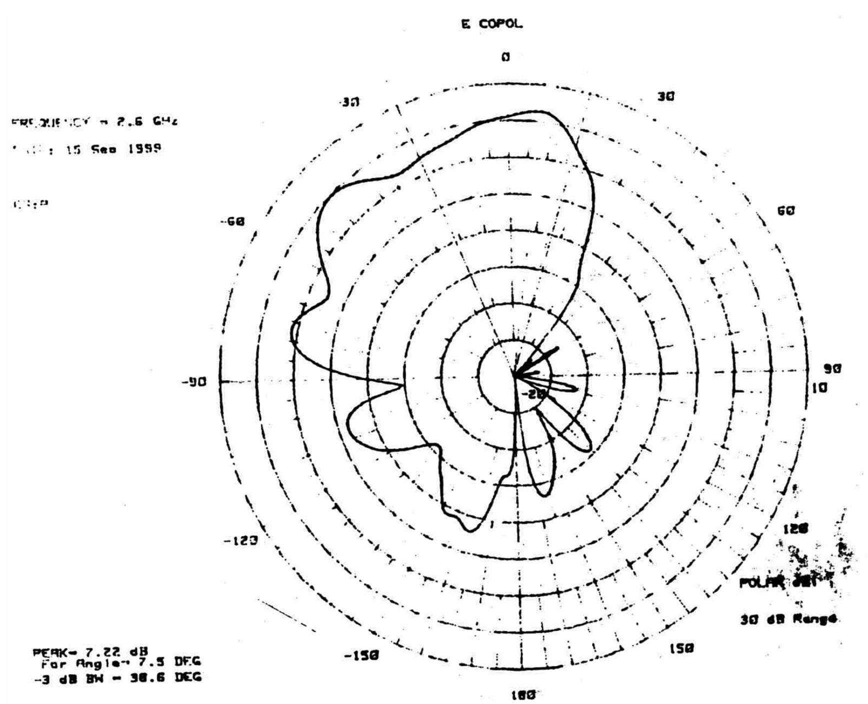

Figure 5. Measured Radiation Pattern of the New Microstrip-Horn Antenna at 2.6 GHz (First Design).

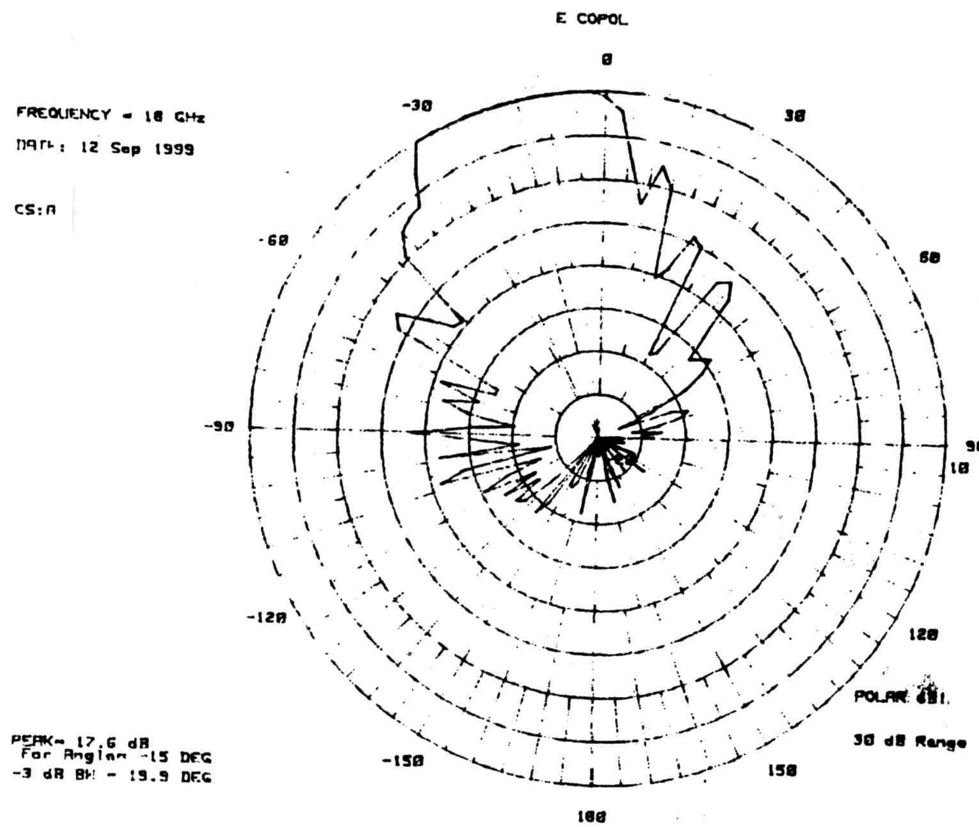

Figure 6. Measured Radiation Pattern of the New Microstrip-Horn Antenna at 18 GHz (First Design).

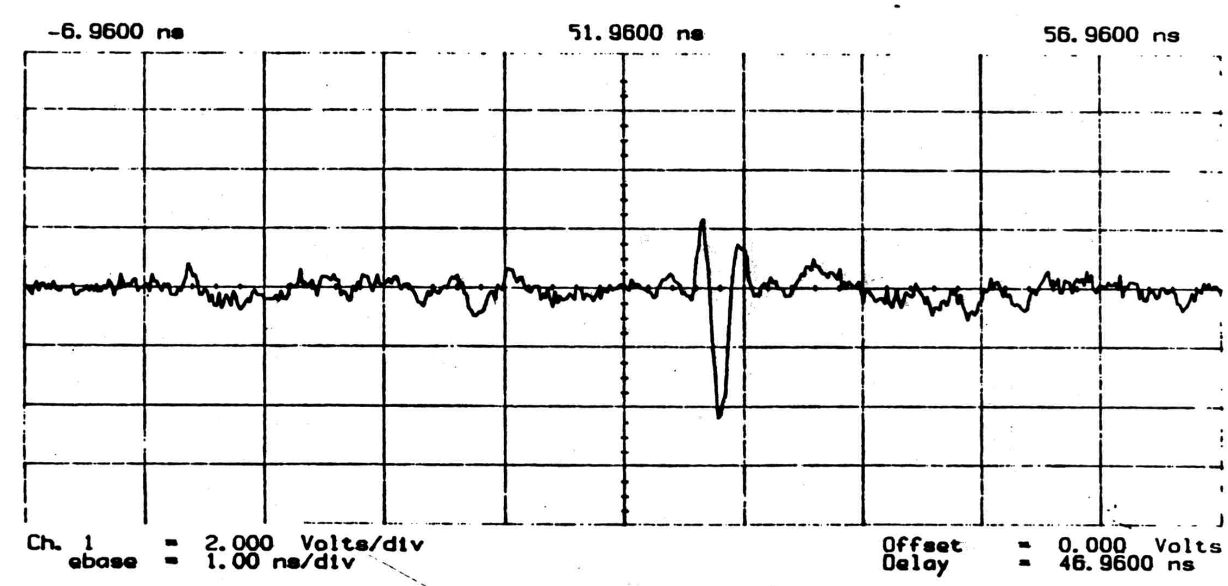

Figure 7. Received Pulse Using the New Microstrip-Horn Antenna (First Design).

The amplitude is not the actual amplitude of the received pulse as attenuators were used in the measurement setup.

The received pulse was obtained using the same 0.33 ns mono-cycle pulse as the transmitting signal. It should be noted that these results were obtained for the initial design only; further optimization will produce better results. As described later, the researchers plan to redesign and optimize the antenna to improve its performance.

3.2 Transmitter

The transmitter consists of a mono-cycle pulse generator and a power amplifier. The researchers purchased the amplifier. The mono-cycle pulse generator has been developed internally. Figures 8 and 9 show the calculated and measured performance of our first design for the new mono-cycle pulse generator. This first prototype achieved good results. This pulse generator is realized using a coplanar wave-guide (transmission line), in which all of the circuit elements are located on one side of the substrate, its benefits being simplicity and low cost.

It is proposed to redesign and optimize this new mono-cycle pulse generator to achieve higher amplitude and minimize ringing.

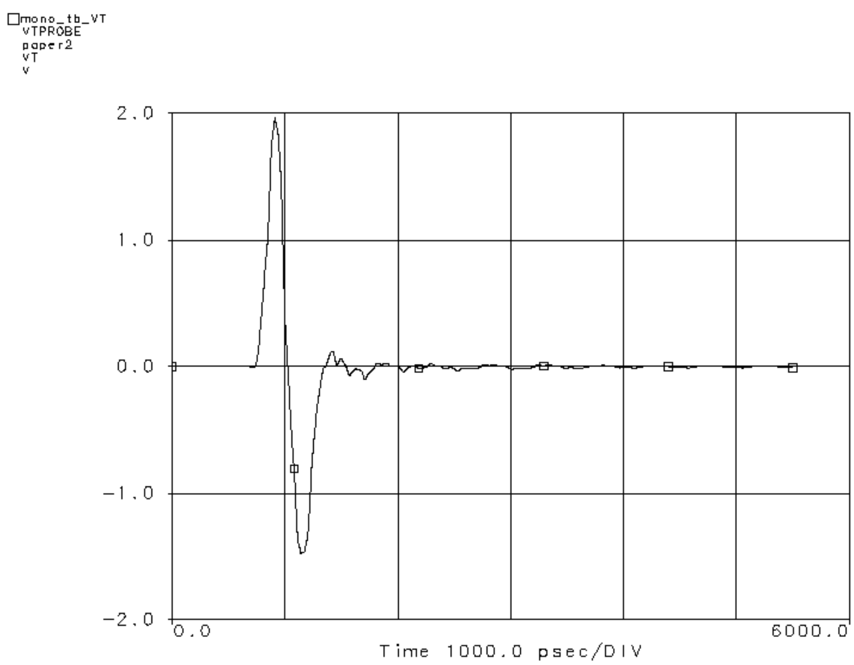

Figure 8. Simulation Result of the New Mono-pulse Generator.

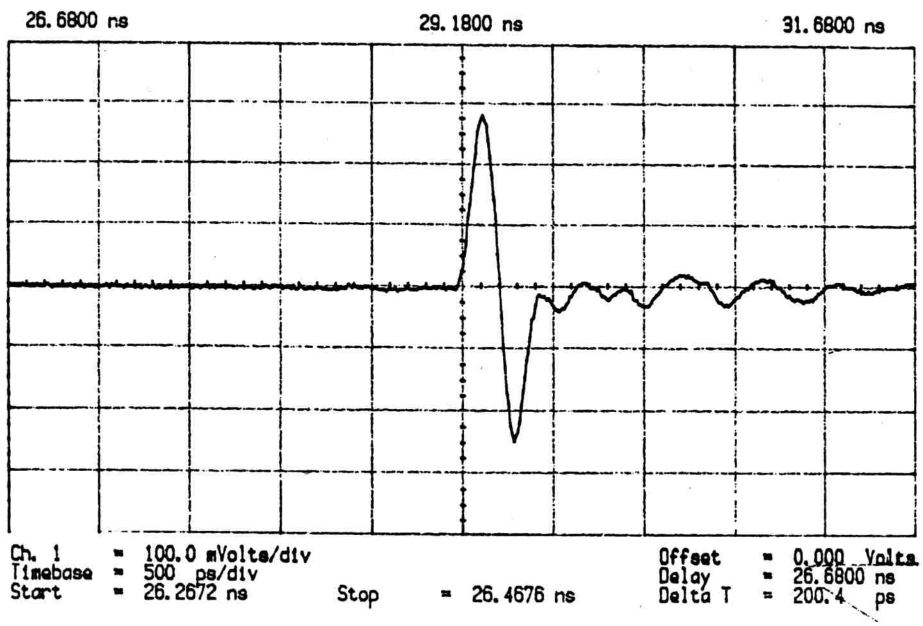

Figure 9. Experimental Result of the New Mono-cycle Pulse Generator.

3.3 Receiver

The researchers developed a new integrated-circuit receiver using sequential or coherent sampling. This sampling scheme has a relatively low sampling rate and is generally used in pulsed subsurface penetrating radar. The receiver has its own local oscillator (LO), pulse generator, and intermediate-frequency (IF) amplifier, making it a complete receiver subsystem. It is completely fabricated using (uni-planar) coplanar wave-guide (CPW) and slot line, in which all of the circuit elements are located on one side of the substrate, which is highly desirable for both simplicity and low cost. These unique advantages are attained because uni-planar structures make it easy to mount solid-state devices; they eliminate via holes and permit one-sided circuit processing. In addition, novel configurations for the sampling head and pulse generator are used to achieve less-distortion sampling pulses and high conversion gain by exploiting the combined advantages of CPW and slot line. The sampling head of the receiver uses a two-diode sampling bridge to make a balanced structure for good inter-port isolations and cancellation of amplitude modulation (AM) noise from the LO. The pulse generator employs a step-recovery diode (SRD) and an ultra-wide-band hybrid junction to create two opposite pulses for gating (or turning on/off) the sampling diodes.

Figure 10 shows a block diagram of the receiver, consisting of a sub-nanosecond pulse generator, hybrid junction, sampling head, LO, and IF amplifier. The main components are the pulse generator, hybrid junction, and sampling head. The pulse generator generates a step function from the LO signal, which is then fed to the hybrid junction to produce two opposite pulses for gating the sampling diodes. The sampling head samples, holds, and converts the radio frequency (RF) signal into an IF signal.

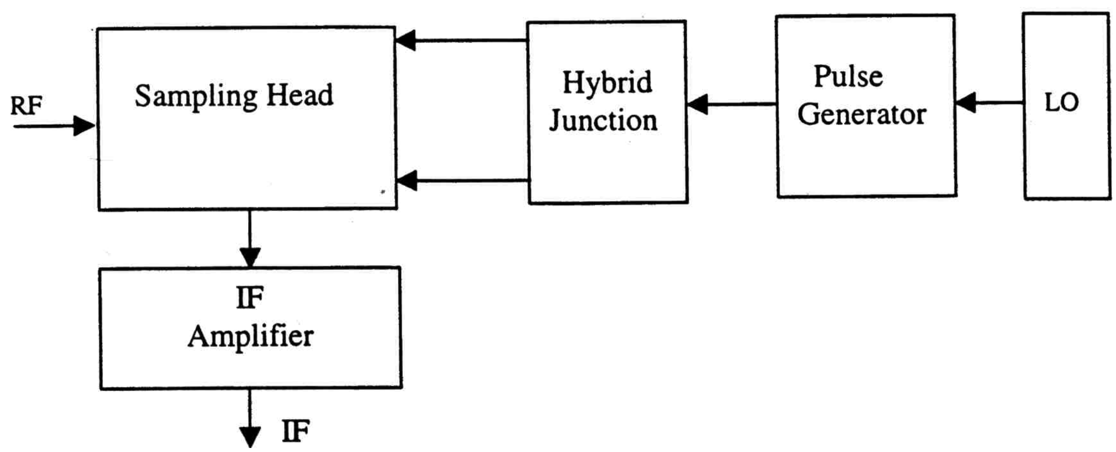

Figure 10. Block Diagram of the Receiver.

Figure 11 is the layout of the complete integrated-circuit receiver including the LO and IF amplifier. All the elements are located on only one side of the substrate. Both the input and output ports are CPW and, thus, are readily interfaced with external components. The LO is a crystal oscillator that generates a square wave of 10 MHz repetition rate with a good frequency stability and low phase noise. The IF amplifier is an analog operational amplifier.

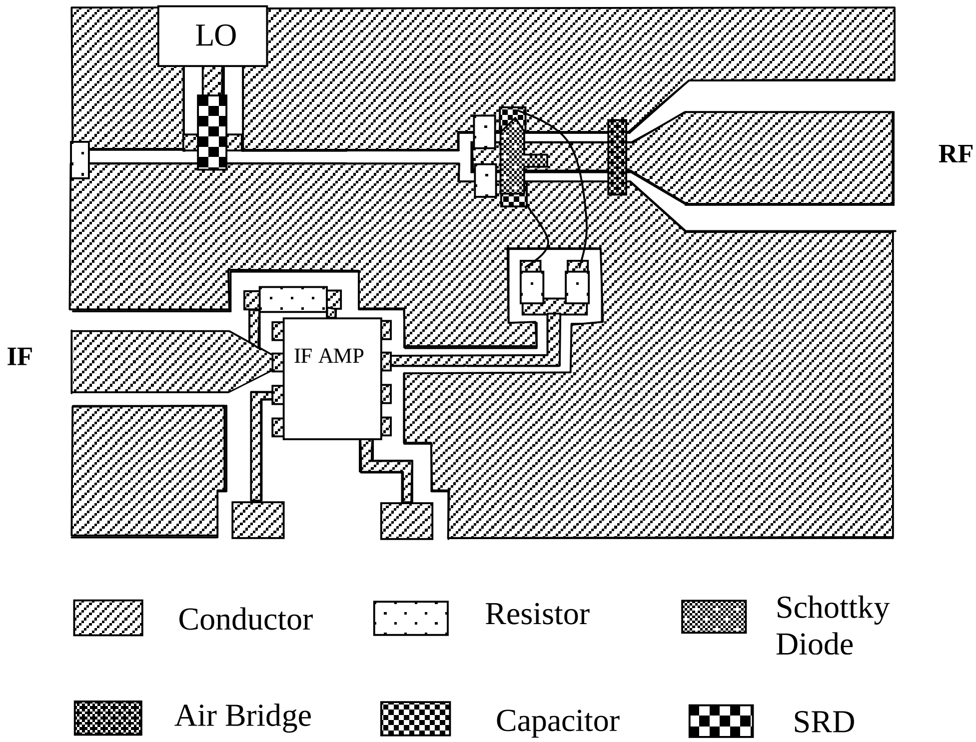

Figure 11. Layout of the Receiver.

Figure 12 displays the measured and simulated conversion gains of the receiver versus RF frequency, showing a 3 dB bandwidth of almost 3 GHz. The down-converted IF signal is about 11 KHz. Figure 13 shows the measured and calculated return losses at the RF port. The measured return loss is more than 15 dB up to 3.5 GHz. As seen in Figures 12 and 13, the measured and calculated results agree reasonably well. Figure 14 shows the measured powers of the fundamental, second, and third harmonics of the output IF signal versus RF input power at 1.5 GHz, which was sampled at a 10 MHz rate. This figure also illustrates typical output linearity and harmonic response of the receiver.

It should be noted that these results were obtained with the first design of the receiver. We expect better performance with further optimizations. We will redesign the receiver to achieve a wider operating bandwidth and higher gain.

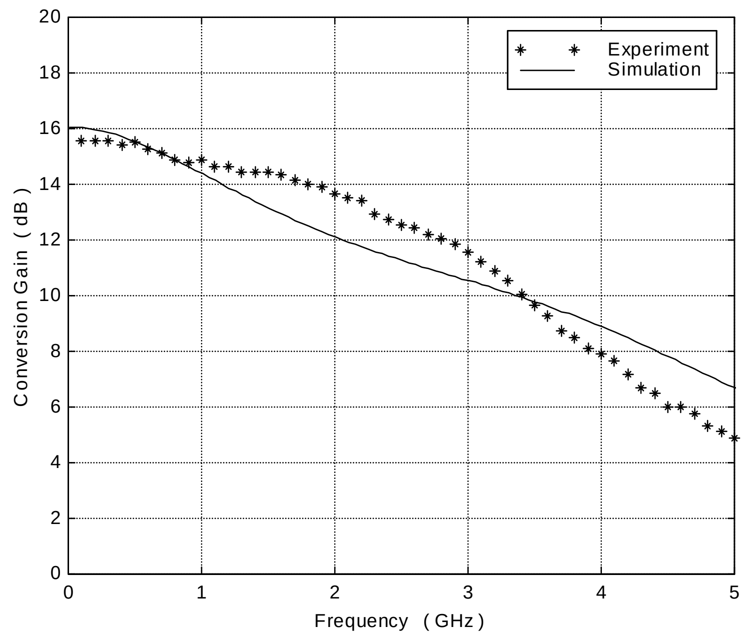

Figure 12. Conversion Gain of the Receiver.

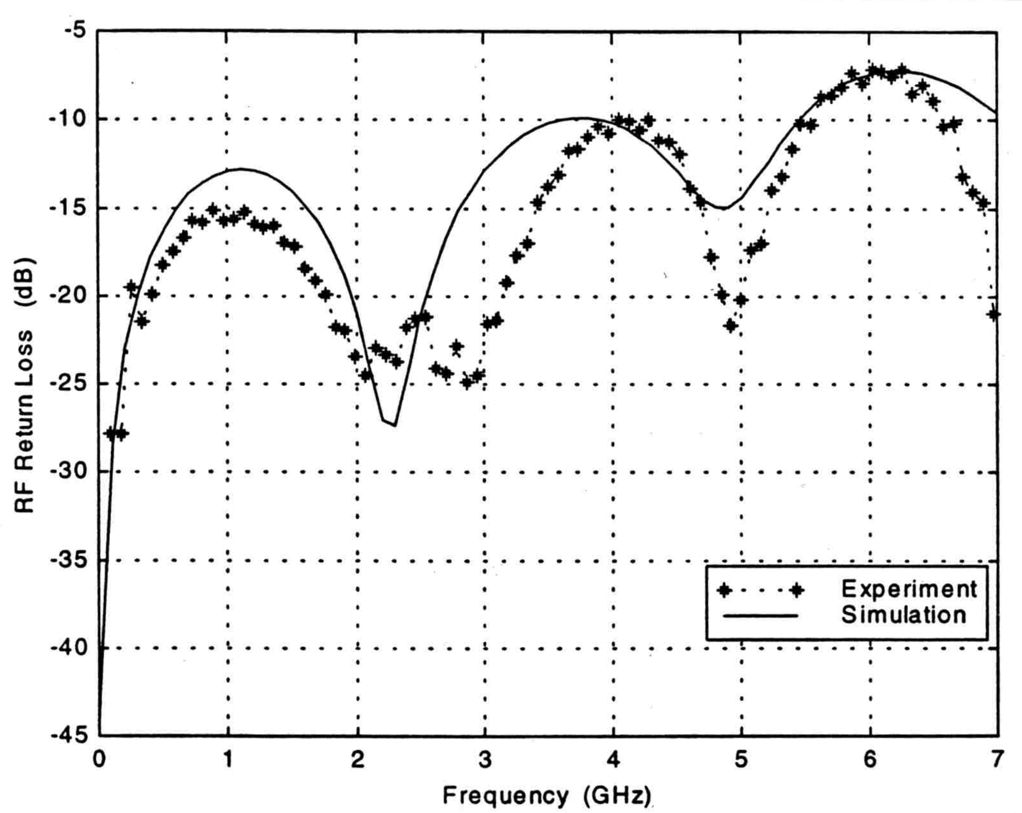

Figure 13. RF Return Loss of the Receiver.

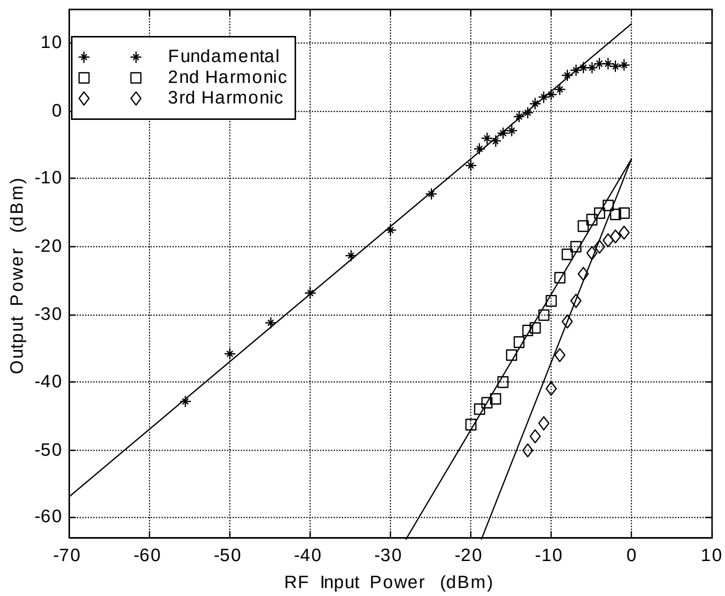

Figure 14. Output Powers of the Receiver Versus RF Input Power.

CHAPTER 4. GPR PERFORMANCE

A first prototype GPR has been assembled using the components described in Chapter 3 and tested in the laboratory at the Texas Transportation Institute. The initial results, as will be shown below, are promising.

Figure 15 shows the received signal that is reflected back from a metal plate. Part A of the received signal is due to coupling between the transmitter and receiver, B represents the reflected signal from the metal plate, and C is from the mismatch and clutter. Future efforts will aim to minimize this clutter level. Figure 16 shows the reflected signal from a 4-inch-thick asphalt layer that is suspended 3.7 inches from the floor. Part A in Figure 16 is from the coupling between the transmitter and receiver, B is due to the reflection from the top layer of the asphalt surface, and C is caused by the boundary between the bottom surface of the asphalt and air.

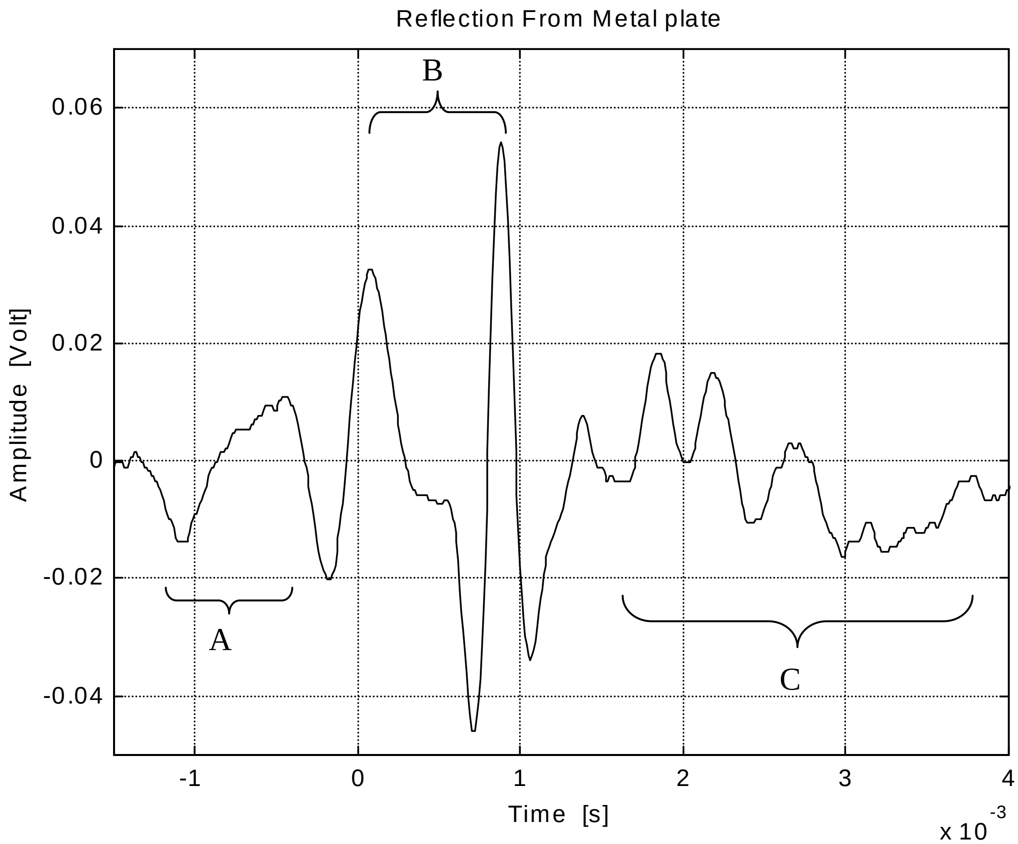

Figure 15. Reflection from a Metal Plate.

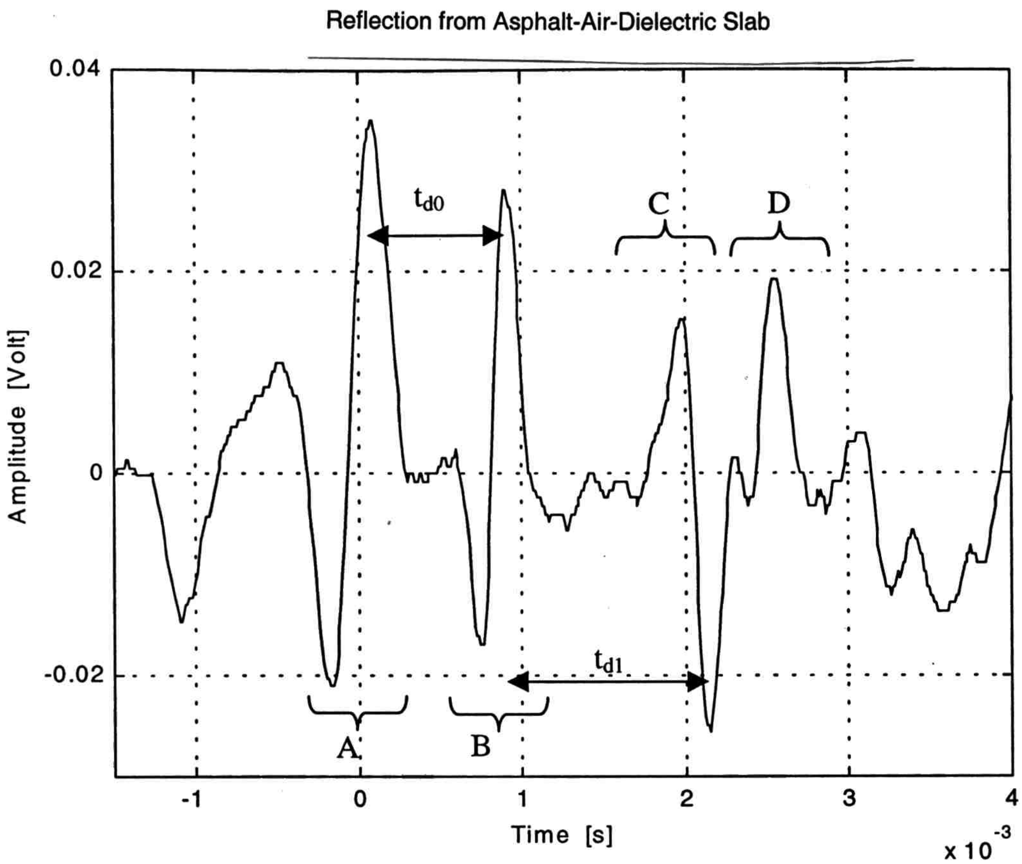

Figure 16. Reflection from an Asphalt Layer Suspended from the Ground.

It should be noted that this performance was obtained with our first GPR prototype. No optimizations of the components and system have been made. We expect that a second-iteration GPR incorporating redesigned components and further optimization of the system will significantly improve the system performance.

CHAPTER 5. CONCLUSIONS AND FUTURE PLAN

We have researched, designed, and tested all necessary components for a 3 GHz GPR prototype. These initial components performed reasonably well in the laboratory. The researchers have also integrated these components to form a first prototype GPR. Although this GPR is only a first-iteration system, it has promising results at 3 GHz, demonstrating the feasibility of the GPR system concept.

To produce a final GPR system that can be used in the field for various pavement applications, the following continuing system development activities are recommended.

- Redesign all the components of the GPR to achieve better performance. Specifically, we will optimize the receiver, mono-pulse generator, and antennas. The receiver will be optimized to achieve a bandwidth up to 10 GHz and higher gain. This is necessary to capture the wide-band signal reflected from a pavement structure to display complete subsurface information. The mono-cycle pulse generator will be redesigned to give higher output power and less ringing. The antenna will be redesigned to have better radiation patterns and less coupling between the transmitting and receiving antennas.
- Redesign the system architecture for better performance. Noise reduction circuitry will be implemented in the receiver to lower the system noise and hence increase the signal-to-noise level.
- Integrate all redesigned components to form a complete integrated-circuit GPR system and evaluate it in the laboratory and field. This final system will have the transmitter and receiver integrated together with the transmitting and receiving antennas on the same substrates using printed circuits. This approach will ensure the miniaturization, low cost, and high efficiency for the GPR. We envision the final system, including the transmitter, receiver, antennas, and electronic circuits, to have an overall size of about 12 inch x 10 inch x 9 inch.